Int. J. Heat Mass Transfer. Vol. 35, No. 9, pp. 2289–2297, 1992
Printed in Great Britain

0017–9310/92 $5.00 + 0.00
Pergamon Press Ltd

Conjugate heat transfer between two natural convections separated by a vertical plate

MIKIO SAKAKIBARA† and HIROSHI AMAYA
Department of Applied Chemistry, Fukui University, Fukui 910, Japan

and

SHIGERU MORI and AKIRA TANIMOTO
Department of Chemistry and Chemical Engineering, Kanazawa University, Kanazawa 920, Japan

(*Received* 6 *February* 1991 *and in final form* 10 *June* 1991)

Abstract—Coupled heat transfer between two laminar natural convection systems separated by a vertical conductive wall is theoretically analyzed, taking account of the two-dimensional thermal conduction in the separating wall. Numerical solutions of temperature fields for both fluid flows are combined with the analytical solution for the wall so as to satisfy the continuity of the temperature and the heat flux at both sides of the conducting wall. Obtained results of the whole temperature field show that the axial conduction effect in the wall is substantial when the wall is thick and has a high thermal conductance, and that axial conduction in the wall is found to relax the interference between the two convections in both fluids. Experiments have been conducted for air–air systems with the conducting wall made of aluminum or glass. Theoretical predictions describe well the experimental temperature distributions, showing the validity of the present analysis.

1. INTRODUCTION

RECENT demands in heat transfer engineering have requested researchers to develop various new types of heat transfer equipments with superior performance, especially compact and light-weight ones. Increasing the need for small-size units, focuses have been cast on the effects of the interaction between developments of the thermal boundary layers in both fluid streams, and of axial wall conduction, which usually degrades the heat exchanger performance.

Concerning the former effect, various types of conjugate heat transfer problems have been studied since the 1970s. They can be roughly classified into the following three groups from the viewpoint of accompanied flows: (A) two adjacent forced convections, (B) forced convection and external natural convection, and (C) two adjacent natural convections. In earlier investigations, the first type of problem had initially been solved because the flow was not greatly influenced by the heat transfer in the usual cases and the equations of motion and energy could be solved separately. However, problems including natural convection were later analyzed because of difficulties in solving the developments of flow and thermal boundary layer simultaneously.

On the coupled heat transfer between a forced convection and the ambient natural convection, Sparrow and Faghri [1] treated theoretically a case with an upward forced flow in a vertical circular tube and the external natural convection induced in the same direction; however, their analysis did not include the wall conduction effect at all.

For two natural convection systems, Lock and Ko [2] studied a problem with a vertical wall of finite thickness. After they transformed fundamental equations by introducing a similarity variable, they obtained numerical results using a finite difference method. Although their analysis assumed that wall conduction is only in the transverse direction, they pointed out that the two-dimensional conduction equation should be employed because axial conduction in the wall would play an important role in such a conjugate problem. Recently, more detailed discussions on the same problem were made by Anderson and Bejan [3] and Viskanta and Lankford [4]. In particular, the latter conducted interferometric experiments and confirmed the validity of their approximated theoretical analysis based on a superposition technique. They also suggested that further investigations are required for cases with the significant effect of axial wall conduction. More recently, research has been extended to geothermal problems [5], energy regenerators [6] and thermal isolation [7]. In major research to date treating any of the above combinations, the wall, if included, is merely considered as a partition without any thermal effect or with a thermal resistance only in the transverse direction.

With respect to the effect of axial wall conduction on the interaction between two forced convections,

†To whom correspondence should be addressed.

NOMENCLATURE

$E(\ )$	objective functions defined by equation (22) or (23)
$F(\ ), G(\ )$	dimensionless interfacial temperature
g	gravitational acceleration [m s^{-2}]
Gr	modified Grashof number, $g\beta(T_{1\infty}-T_{2\infty})H^3/\nu^2$
Gr_x	local Grashof number, $g\beta(T_{1\infty}-T_{2\infty})x^3/\nu^2$
H	height of conducting wall [m]
K	dimensionless thermal conductivity of wall, k_w/k
k	thermal conductivity [W m^{-1} K^{-1}]
L^*	aspect ratio of wall, δ/H
Nu	local Nusselt number defined by equation (24)
P	parameter defined by equation (26)
Pr	Prandtl number, ν/α
T	temperature [K]
U	dimensionless velocity in the vertical direction, uH/ν
u	velocity component in the vertical direction [m s^{-1}]
V	dimensionless velocity in the horizontal direction, vH/ν
v	velocity component in the horizontal direction [m s^{-1}]
X	dimensionless coordinate, x/H
x	vertical coordinate [m]
Y	dimensionless coordinate, y/H
y	horizontal coordinate [m]
Y_w	dimensionless coordinate, y_w/δ
y_w	horizontal coordinate for the wall [m].

Greek symbols

α	thermal diffusivity [m^2 s^{-1}]
β	thermal expansion coefficient [K^{-1}]
δ	thickness of conducting wall [m]
Θ	dimensionless fluid temperature, $(T-T_{2\infty})/(T_{1\infty}-T_{2\infty})$
Θ_w	dimensionless wall temperature, $(T_w-T_{2\infty})/(T_{1\infty}-T_{2\infty})$
ν	kinematic viscosity [m^2 s^{-1}]
ν_i	coefficient in power series, to be determined
ξ	dummy variable
τ_i	coefficient in power series, to be determined.

Subscripts

w	wall
1	hot fluid (Fluid 1)
2	cold fluid (Fluid 2)
∞	outside of boundary layer.

a theoretical analysis was performed on a counter-current parallel-plate heat exchanger with laminar flows by Mori *et al.* [8]. They found that axial conduction significantly relaxes the thermal interaction between the two convection systems.

In the present paper, a theoretical analysis on counter-current natural convection systems with two-dimensional conduction in the separating finite wall is reported, following the above-mentioned suggestions by Lock and Ko [2] and Viskanta and Lankford [4]. Two numerical solutions for both natural convections and an analytical solution for the wall conduction are combined to obtain the final solutions so as to fit the conjugate boundary conditions at both interfaces. Numerical results are shown for a system symmetrical with respect to the center of the conducting wall, and the results of the distributions of the interfacial temperature and the local Nusselt number are presented to show the significant wall conduction effect. Experimental temperature profiles obtained for air–air systems with an aluminum or a glass wall are compared with the theoretical predictions in order to show the validity of the present analysis.

2. THEORETICAL ANALYSIS

Consider two stagnant fluids separated by an infinite, vertical wall with a heat-conducting section of height H. Spaces extending at both sides of the wall are assumed to be sufficiently large so as to be regarded as semi-infinite. When the two fluids are at different temperatures, $T_{1\infty}$ and $T_{2\infty}$, natural convection is induced downwards in hot fluid (Fluid 1) and upwards in cold fluid (Fluid 2). Such a situation is shown schematically in Fig. 1 with the coordinate systems used in the following analysis.

The developments of the thermal and the hydrodynamic boundary layers depend on the temperature

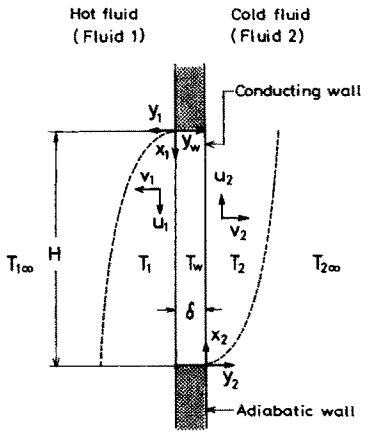

FIG. 1. Analytical model.

at the wall–fluid interface. However, the interfacial temperature cannot be determined straightforwardly under any prescribed conditions and has to be determined as a result of the conjugate heat transfer from the hot fluid to the cold fluid through the conducting wall. Consequently, we must solve the fundamental equations for two natural convection systems and the wall simultaneously. Since the problem is very complicated, the following simplifications are introduced:

(i) Boussinesq and boundary layer approximations are applicable to both natural convections;

(ii) the axial conduction is negligible for both fluid streams;

(iii) all the physical properties are constant except for the density in the buoyancy term in the momentum equation;

(iv) the problem is two-dimensional and the steady state is attained.

2.1. *Formulation*

To formulate the present problem, the dimensionless variables and the parameters are defined as

$$X = x/H, \quad Y = y/H, \quad Y_w = y_w/\delta, \quad U = uH/\nu,$$
$$V = vH/\nu, \quad \Theta = (T-T_{2\infty})/(T_{1\infty}-T_{2\infty}),$$
$$\Theta_w = (T_w-T_{2\infty})/(T_{1\infty}-T_{2\infty}),$$
$$Gr = \frac{g\beta(T_{1\infty}-T_{2\infty})H^3}{\nu^2}, \quad K = \frac{k_w}{k},$$
$$L^* = \frac{\delta}{H}, \quad Pr = \nu/\alpha.$$

Furthermore, to specify the quantities relating to Fluid 1 and Fluid 2, subscripts 1 and 2 are used.

By using the above dimensionless groups, the problem is represented by the following equations and conditions:

For hot fluid (Fluid 1)

$$\frac{\partial U_1}{\partial X_1} + \frac{\partial V_1}{\partial Y_1} = 0 \tag{1}$$

$$U_1\frac{\partial U_1}{\partial X_1} + V_1\frac{\partial U_1}{\partial Y_1} = Gr_1(1-\Theta_1) + \frac{\partial^2 U_1}{\partial Y_1^2} \tag{2}$$

$$U_1\frac{\partial \Theta_1}{\partial X_1} + V_1\frac{\partial \Theta_1}{\partial Y_1} = \frac{1}{Pr_1}\frac{\partial^2 \Theta_1}{\partial Y_1^2} \tag{3}$$

with boundary conditions

$$\text{at } X_1 = 0, \quad U_1 = 0, \quad \Theta_1 = 1 \tag{4}$$

$$\text{at } Y_1 = 0, \quad U_1 = 0, \quad V_1 = 0, \quad \Theta_1 = F(X_1) \tag{5}$$

$$\text{at } Y_1 = \infty, \quad U_1 = 0, \quad \Theta_1 = 1. \tag{6}$$

For cold fluid (Fluid 2)

$$\frac{\partial U_2}{\partial X_2} + \frac{\partial V_2}{\partial Y_2} = 0 \tag{7}$$

$$U_2\frac{\partial U_2}{\partial X_2} + V_2\frac{\partial U_2}{\partial Y_2} = Gr_2\Theta_2 + \frac{\partial^2 U_2}{\partial Y_2^2} \tag{8}$$

$$U_2\frac{\partial \Theta_2}{\partial X_2} + V_2\frac{\partial \Theta_2}{\partial Y_2} = \frac{1}{Pr_2}\frac{\partial^2 \Theta_2}{\partial Y_2^2} \tag{9}$$

with boundary conditions

$$\text{at } X_2 = 0, \quad U_2 = 0, \quad \Theta_2 = 0 \tag{10}$$

$$\text{at } Y_2 = 0, \quad U_2 = 0, \quad V_2 = 0, \quad \Theta_2 = G(X_2) \tag{11}$$

$$\text{at } Y_2 = \infty, \quad U_2 = 0, \quad \Theta_2 = 0. \tag{12}$$

For the wall

$$L^{*2}\frac{\partial^2 \Theta_w}{\partial X_1^2} + \frac{\partial^2 \Theta_w}{\partial Y_w^2} = 0 \tag{13}$$

with boundary conditions

$$\text{at } X_1 = 0 \text{ and } 1, \quad \partial\Theta_w/\partial X_1 = 0 \tag{14}$$

$$\text{at } Y_w = 0, \quad \Theta_w = F(X_1) \tag{15}$$

$$\text{at } Y_w = 1, \quad \Theta_w = G(X_2). \tag{16}$$

The conjugate boundary conditions at the interface are

$$\text{at } Y_1 = 0 \quad (\text{or } Y_w = 0),$$
$$\frac{\partial \Theta_1}{\partial Y_1} = -\frac{K_1}{L^*}\frac{\partial \Theta_w}{\partial Y_w} \tag{17}$$

$$\text{at } Y_w = 1 \quad (\text{or } Y_2 = 0),$$
$$-\frac{K_2}{L^*}\frac{\partial \Theta_w}{\partial Y_w} = -\frac{\partial \Theta_2}{\partial Y_2}. \tag{18}$$

In the foregoing equations (5), (11), (15) and (16), the unknown interfacial temperatures on the hot and cold fluid sides are conveniently expressed by $F(X_1)$ and $G(X_2)$, respectively.

2.2. *Solution procedure*

Such boundary layer equations as mentioned above are often analyzed by introducing similarity variables. However, the similarity solution is successfully obtained only in the case with a boundary condition of constant temperature or constant heat flux at the fluid–wall interface. Furthermore, the superposition of solutions for some simplified problems is not adequate for the present case because of the nonlinearity of the fundamental partial differential equations. Usually, an analysis of the problem under the boundary condition with a change in wall temperature or heat flux is performed by the local nonsimilarity solution [9], but this method would be too complicated to apply directly to the present multi-region problem. Therefore, the boundary layer equations for each of the fluids were solved numerically in the present work by applying the finite difference method [10].

As determination of the interfacial temperatures is not easy to satisfy the continuities of temperature and heat flux at each interface, the interfacial temperatures

to be determined are expanded to the following power series of X_1 or X_2 with unknown coefficients

$$F(X_1) = 1 + v_0 + \sum_{i=1}^{\infty} v_i X_1^i, \tag{19}$$

$$G(X_2) = \tau_0 + \sum_{i=1}^{\infty} \tau_i X_2^i. \tag{20}$$

If the coefficients v_i and τ_i are specified, the set of finite difference equations will be solved by iterative calculation for each fluid independently.

On the other hand, the heat conduction equation in the wall, equation (13), is solved analytically for prescribed interfacial temperature distributions as follows [8]:

$$\Theta_w = (1 - Y_w)\int_0^1 F(\xi)\,d\xi + Y_w \int_0^1 G(1-\xi)\,d\xi + 2\sum_{n=1}^{\infty} \frac{\cos(n\pi X_1)}{\sinh(n\pi L^*)} \left(\sinh\{n\pi L^*(1-Y_w)\} \times \int_0^1 F(\xi)\cos(n\pi\xi)\,d\xi + \sinh(n\pi L^* Y_w) \times \int_0^1 G(1-\xi)\cos(n\pi\xi)\,d\xi \right). \tag{21}$$

Coupling the solutions for all the regions obtained in the ways mentioned above is carried out by the following procedure. First, the unknown coefficients, v_i and τ_i, are assumed roughly. Then the two sets of finite difference equations for both boundary layer flows are calculated independently. The wall temperature is then estimated from equation (21). Next, the dimensionless heat fluxes calculated from the obtained temperature distributions for three regions are substituted into the following objective functions, which are defined on the basis of the conjugate boundary conditions, equations (17) and (18):

$$E_1(v_0, v_1, \ldots) = \sum_{j=1}^{N} \left| \left(\frac{\partial \Theta_1}{\partial Y_1}\right)_{Y_1=0,\, X_1=X_j} + \frac{K_1}{L^*}\left(\frac{\partial \Theta_w}{\partial Y_w}\right)_{Y_w=0,\, X_1=X_j} \right| \tag{22}$$

$$E_2(\tau_0, \tau_1, \ldots) = \sum_{j=1}^{N} \left| \left(\frac{\partial \Theta_2}{\partial Y_2}\right)_{Y_2=0,\, X_2=X_j} - \frac{K_2}{L^*}\left(\frac{\partial \Theta_w}{\partial Y_w}\right)_{Y_w=1,\, X_1=1-X_j} \right|. \tag{23}$$

In order to minimize the objective functions $E_1(v_0, v_1, \ldots)$ and $E_2(\tau_0, \tau_1, \ldots)$, the assumed values of the coefficients v_i and τ_i are systematically adjusted by applying the simplex method. After the values of the coefficients have converged, the temperature fields in both fluids and the wall are established. The local Nusselt number, based on the temperature field obtained for the hot fluid side, is estimated by the following definition:

$$Nu_1 = \frac{-\left(\frac{\partial \Theta_1}{\partial Y_1}\right)_{Y_1=0}}{(\Theta_1)_{Y_1=0} - 1} X_1. \tag{24}$$

In the present calculations, equations (19) and (20) were truncated at the term of X_1^3 or X_2^3. For each of the objective functions, the errors in the trial were evaluated at nine points, that is, at X_1 or $X_2 = 0.1$–0.9 at intervals of 0.1. The iteration was repeated till both E_1 and E_2 became less than a few percent of the dimensionless interfacial heat flux. To calculate the flow and the temperature fields, the initial value at every grid point was given by the analytical solution presented by Sparrow [11]. The increments in the X and Y directions for the finite difference equations were 0.05 and 0.0025, respectively. The convergence criterion was set to be 10^{-3} in the maximum difference between the results of the nth and $(n+1)$th trials for all the grid points. With these increments and the convergence criterion, a model problem with the condition of constant wall temperature was solved and the result was confirmed to give good agreement with the well-known similarity solution except in a region very close to the leading edge.

In addition, in the case where the axial wall conduction is neglected, the conjugate boundary condition at the interfaces is given by the following in dimensionless form:

$$\frac{1}{K_1}\left(\frac{\partial \Theta_1}{\partial Y_1}\right)_{Y_1=0} = \frac{1}{L^*}((\Theta_1)_{Y_1=0} - (\Theta_2)_{Y_2=0}) = -\frac{1}{K_2}\left(\frac{\partial \Theta_2}{\partial Y_2}\right)_{Y_2=0}. \tag{25}$$

In this case also, numerical calculations can be made in a similar manner as mentioned above.

3. NUMERICAL RESULTS AND DISCUSSION

When a system of interest consists of two different kinds of fluids, there are many parameters to describe the effect of each fluid on heat transfer characteristics. Therefore, in the present report, a case where two working fluids have the same physical properties is examined in detail. In this case, the temperature fields become completely symmetrical with respect to the center point of the conducting wall. Accordingly, the heat transfer characteristics will be examined and discussed mainly for the hot fluid side.

Conditions prescribed for numerical calculations are as follows: $Pr(= Pr_1 = Pr_2) = 0.7$, $10^6 \leqslant Gr (= Gr_1 = Gr_2) \leqslant 10^8$, $1 \leqslant K(= K_1 = K_2) \leqslant 1000$, $0.001 \leqslant L^* \leqslant 0.5$.

Initially, to confirm the validity of the procedure for numerical calculations, the interfacial temperature for the case where the axial wall conduction is negligible is estimated by using the conjugate boundary condition, equation (25), and is compared with the result of Viskanta and Lankford. In their study, the

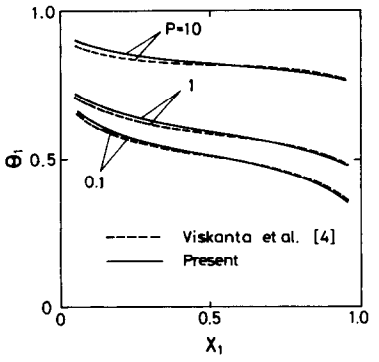

FIG. 2. Comparison of numerical results with those of Viskanta: interfacial temperature on the hot fluid side ($Pr = 0.7$, $Gr = 10^7$, $L^* = 0.1$).

following dimensionless parameter was employed to represent the heat transfer characteristics:

$$P = \frac{L^*}{K}(Gr\,Pr)^{1/4}. \tag{26}$$

Numerical calculations are carried out for $P = 0.1$, 1.0 and 10 by changing the value of K under the conditions of $Pr = 0.7$, $Gr = 10^7$ and $L^* = 0.1$. Figure 2 compares the obtained interfacial temperatures on the hot fluid side and their solutions represented by broken lines. Despite a slight deviation for $P = 1$, on the whole both results agree well, showing the validity of the present numerical analysis.

The dependence of the interfacial temperature and the local Nusselt number on the parameter K are shown in Fig. 3. The other parameters are fixed as $Pr = 0.7$, $Gr = 10^7$ and $L^* = 0.1$. The broken curves in the upper graph are the result for the one-dimensional analysis without axial wall conduction. In the lower graph, the local Nusselt numbers under the conditions of constant wall temperature and constant wall heat flux are also shown for reference. The local Nusselt numbers for $K = 1$–100 obtained by the one-dimensional analysis were in agreement with those for the exact results, and that for $K = 1000$ almost agreed with the exact case for $K = 100$.

The comparison of the interfacial temperature by the present method with that obtained by the one-dimensional analysis shows that the axial wall conduction has a significant effect on the interfacial temperature when K is large and that the assumption of wall conduction only in the transverse direction holds in cases for a comparatively small value of K. In the upper graph, the interfacial temperature curve shows a sigmoid change with an increase in X_1 for $K = 100$. However, for $K = 1$, the change becomes rather moderate, and for $K = 1000$ the curve is linear, flat and close to 0.5. In the lower graph, the local Nusselt number for $K = 100$ is the highest, especially in the large X_1 region. However, for $K = 1000$, the local Nusselt number decreases in the whole region, and is close to the curve for the case with the constant wall temperature. On the other hand, the curve for $K = 1$ is close to that for the case with the constant wall heat flux. For $K = 10000$, though numerical results were not obtained because of poor convergence, the wall temperature will uniformly approach 0.5 and consequently the local Nusselt number will become much closer to that of the constant wall temperature case.

To clarify the effect of axial wall conduction, the temperature profile in the hot fluid and the conducting wall is shown in Fig. 4 for the case at $K = 1000$ and compared with that calculated for the one-dimensional case. A significant difference between these results appears in the wall and in the vicinity of the wall at $X_1 = 0.1$ and 0.9. The discrepancies in the temperature gradient in the neighborhood of the lead-

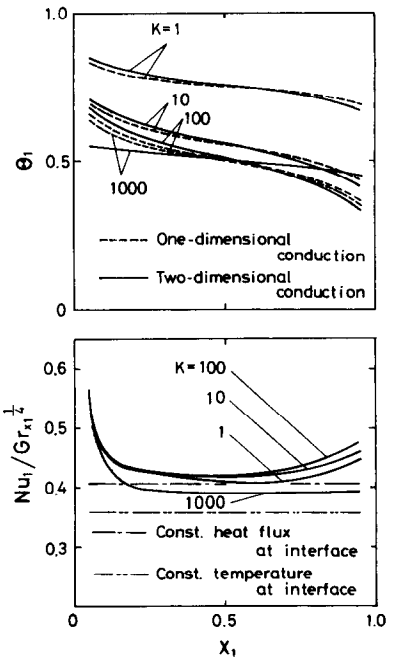

FIG. 3. Interfacial temperature and local Nusselt number on the hot fluid side ($Pr = 0.7$, $Gr = 10^7$, $L^* = 0.1$).

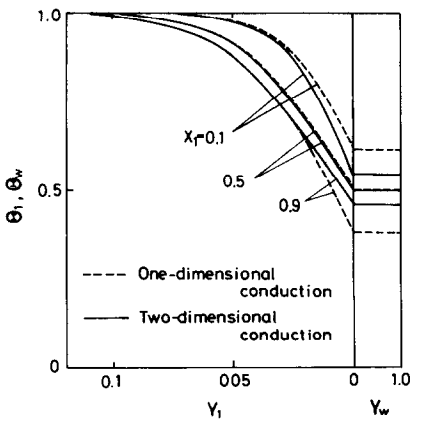

FIG. 4. Temperature profile in the hot fluid and the wall ($Pr = 0.7$, $Gr = 10^7$, $K = 1000$, $L^* = 0.1$).

ing edge and the trailing edge are attributed to the substantial interaction between two natural convections.

The above behaviors of the interfacial temperature, the local Nusselt number and the temperature profile in Figs. 3 and 4 can be explained on the whole as follows. At $K = 100$, the interfacial temperature is almost 0.5 at about $X_1 = 0.5$ and nearly equal to that on the other side. This means that the wall resistance is negligibly small, and that the uneven conductance distribution caused by the developments of the thermal and the hydrodynamic boundary layers in the vicinity of the conducting wall affects almost directly the boundary layer development in the opposite direction in the fluid on the other side. Thus the results for $K = 100$ show the most clear interaction between both sides' natural convections. At $K = 1000$, the thermal resistance in the transverse direction is extremely small; consequently, axial conduction in the wall becomes significant to relax the unevenness of the wall temperature. At $K = 1$, the wall resistance predominates over the overall heat transfer rate and the unevenness of the convective conductance in both fluids loses its significance in the whole heat transfer process. Therefore, the wall conduction in the transverse direction becomes most important, compared to that in the longitudinal direction. Thus the situation approaches the problem with the constant wall heat flux.

The dependences of the interfacial temperature and the local Nusselt number on the parameter L^* are shown in Fig. 5 for $Pr = 0.7$, $Gr = 10^7$ and $K = 10$.

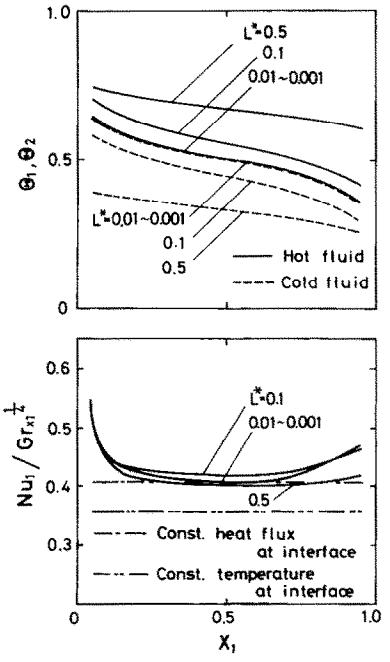

FIG. 5. Interfacial temperature on both fluid sides and local Nusselt number on the hot fluid side ($Pr = 0.7$, $Gr = 10^7$, $K = 10$).

The broken curve in the upper graph is the interfacial temperature on the cold fluid side. In the lower graph of the local Nusselt number, the results for the cases of the constant wall temperature and the constant wall heat flux are also shown.

In general, the effect of the parameter L^* on the heat transfer is similar to that of K. Concerning the local Nusselt number, such a tendency can be observed, that is, an increase in L^* seems to correspond to an increase in K, and the curve becomes largest at about $L^* = 0.1$. However, the interfacial temperature of the hot fluid is high in the full range of X_1 for a large value of L^* and different from the effect of K, and the curve changes its shape from sigmoid to linear. When L^* is specified at any fixed X_1, the difference between $\Theta = 1$ and the solid line curve corresponds roughly to the thermal resistance in the transverse direction of the hot fluid side convection; the difference between the solid and the broken line curves to that of wall conduction; and the difference between the broken line curve and $\Theta = 0$ to the cold fluid side convection. Therefore, from the graph we can easily understand that wall conduction can be neglected for $L^* \leqslant 0.01$ because both side interfacial temperatures agree with each other. This result means that the interaction between two natural convections becomes significant. For an extremely large value of L^*, such as $L^* = 0.5$, the interfacial temperature has a linear distribution along X_1; however, its inclination does not become so small as in the case with $K = 1000$ shown in Fig. 3. This implies that the local Nusselt number does not approach the curve for the case with the constant wall temperature, even for a large value of L^*.

Finally an example of results in the high Grashof number region is given in Fig. 6 for $Gr = 10^8$, where the values of the other parameters are specified as the same as in Fig. 5. The difference of the graph from Fig. 5 in the interfacial temperature is that the effect of L^* becomes more substantial and even at $L^* = 0.5$ the shape of the curve still remains sigmoid, as well as the other curves for smaller values of L^*. In contrast with the interfacial temperature, the local Nusselt number is less affected by L^*. For all the values of L^*, the obtained distributions have almost the same concave curve except for the variations in the large X_1 region and indicate equally the interaction effect between two natural convections.

4. EXPERIMENTAL

The experimental apparatus employed was similar to that reported by Viskanta and Lankford. The apparatus consists of two copper boxes, and the two sides are made of acrylic resin. The dimensions of these boxes are 95 cm height, 43 cm width and 48 cm depth. Each box was covered with a jacket made of an acrylic resin plate. The two boxes were coupled with a 20 mm thick separating board. The board was composed of a core of plywood board 12 mm thick

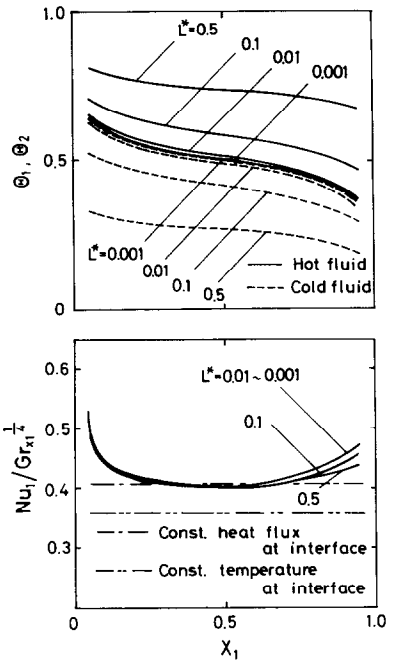

FIG. 6. Interfacial temperature on both fluid sides and local Nusselt number on the hot fluid side ($Pr = 0.7$, $Gr = 10^8$, $K = 10$).

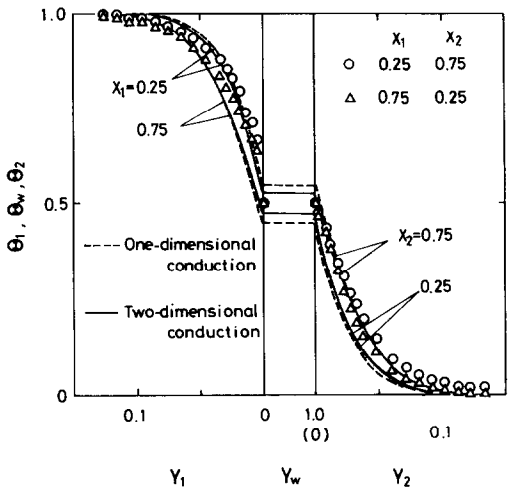

FIG. 7. Temperature profile in fluids and wall (aluminum wall; $Pr = 0.71$, $Gr = 1.05 \times 10^7$, $K = 4600$, $L^* = 0.100$, $T_{1\infty} = 302.7$ K, $T_{2\infty} = 292.5$ K).

and a covering plate of 4 mm thick balsa on both sides. Air was used as both working fluids. A conducting wall 20 cm square and 20 mm thick was placed at the center of the separating board. As materials of the conducting wall, two representative ones with high and low thermal conductivities were used: aluminum alloy and Pyrex glass. To maintain the stagnant air in each enclosed space at a different specified temperature, water was circulated to the jacket through a constant temperature bath. The outside of the apparatus was completely covered with foamed polystyrene to avoid thermal interference from the surroundings.

After the steady state was attained, the surface temperature of the conducting wall was measured by C–C thermocouples of 0.1 mm diameter attached on each side surface at five points at intervals of 40 mm. The temperature profiles in two natural convections were also measured by a C–C thermocouple of 0.1 mm diameter which was tightly stretched between two points of a Y-shaped, thin glass probe. The probe was mounted on a micrometer traverser and a vernier caliper to accomplish accurate positioning. All temperature measurements were performed along the vertical center line of the conducting wall to minimize the influence of the side wall.

The air temperature in one side box was maintained at about room temperature and the other was specified about 10 or 15°C higher or lower than it.

Typical experimental temperature profiles in the transverse direction are shown in Figs. 7 and 8 for the aluminum and glass test walls, respectively. In comparison to the experimental data, theoretical predictions are also given in these figures, calculated not only by the exact analysis but also by the one-dimensional one as in Viskanta's analysis. The former theoretical result is indicated by a solid line and the latter by a broken line.

From Fig. 7 for the aluminum wall, we can observe that the experimental wall temperature does not change in either the transverse or axial direction and is almost constant. Such a situation is simulated fairly well by the theoretical prediction with the exact wall condition, compared with that calculated for the one-dimensional case. This is because axial conduction in the aluminum wall with the high thermal conductivity plays an important role in flattening out the temperature variation induced by the developing boundary layer. On the other hand, in Fig. 8 for the glass wall, both theoretical curves agree very well, showing the validity of the one-dimensional analysis. The exact

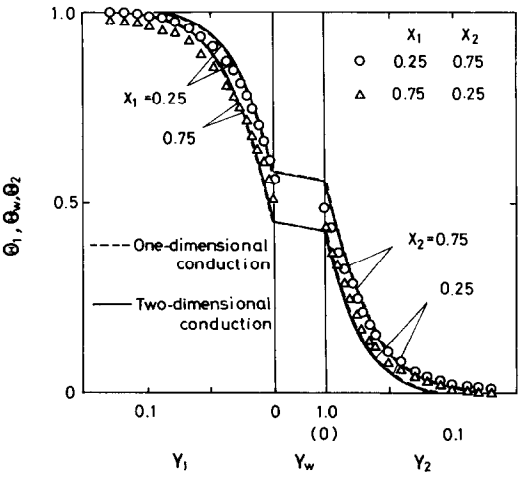

FIG. 8. Temperature profile in fluids and wall (Pyrex glass wall; $Pr = 0.71$, $Gr = 1.09 \times 10^7$, $K = 42.0$, $L^* = 0.100$, $T_{1\infty} = 291.6$ K, $T_{2\infty} = 282.5$ K).

theoretical prediction is in good agreement with the experimental data, as well as in the case with the aluminum wall.

On the whole, the usefulness and validity of the present analysis was verified through the fact that the theoretical prediction of the temperature profile agreed well with the experimental data. However, the following two points were noticed in every experimental result. First, the experimental data tended to deviate a little from the exactly predicted curve in the region far from the conducting wall in both graphs. This would be caused by recirculation flow induced slightly in the test chamber due to its finiteness. Second, the wall temperature obtained by the experiments always changed less in the axial direction, even in comparison with the exact prediction. This phenomenon might be brought about by the effect of the wooden separating wall in which the conducting test wall was installed. Although the thermal conductivity of the wooden wall is smaller than that of the test plate, its total surface area would be considerably larger. Thus the wooden wall might promote the behavior of the conducting wall to ease the local temperature change caused by the developing boundary layer in the vicinities of the conducting wall surfaces.

5. CONCLUSION

A conjugate problem of heat transfer between two laminar natural convections and a finite vertical wall separating them was analyzed theoretically by combining the two numerical solutions for the convections and the analytical one for the wall, in which the thermal conduction in the wall was taken into account in not only the transverse but also the axial directions.

Numerical calculations were performed for a case where the same fluid was employed as both working fluids, and the temperature fields and the local Nusselt number were obtained. The results showed that the ratio of thermal conductivities of the wall and the fluid and the dimensionless thickness of the conducting wall influence substantially the interactive heat transfer between two natural convections induced countercurrently on both sides of the wall. The wall behaves as a buffer for the thermal interaction between the developing boundary layers. Consequently, when the thermal conductivity is high and/or the wall is very thick, the thermal interaction between two natural convections is relaxed and the interfacial temperature tends to have a flat distribution along the wall, where the axial wall conduction plays an important role. In such a case, the treatment simplified as the constant wall temperature became valid.

Experiments were also carried out for air–air systems with conducting walls of aluminum and glass. The observed temperature profiles agreed fairly well with the theoretical predictions calculated by the present analysis.

Acknowledgements—The aluminum test pieces used in these experiments were supplied by Nippon Light Metal Co. Ltd.

REFERENCES

1. E. M. Sparrow and M. Faghri, Fluid-to-fluid conjugate heat transfer for a vertical pipe—internal forced convection and external natural convection, *J. Heat Transfer* **102,** 402–407 (1980).
2. G. S. H. Lock and R. S. Ko, Coupling through a wall between two free convection systems, *Int. J. Heat Mass Transfer* **16,** 2087–2096 (1973).
3. R. Anderson and A. Bejan, Natural convection on both sides of a vertical wall separating fluids at different temperatures, *J. Heat Transfer* **102,** 630–635 (1980).
4. R. Viskanta and D. W. Lankford, Coupling of heat transfer between two natural convection systems separated by a vertical wall, *Int. J. Heat Mass Transfer* **24,** 1171–1177 (1981).
5. R. Anderson and A. Bejan, Heat transfer through single and double vertical walls in natural convection: theory and experiment, *Int. J. Heat Mass Transfer* **24,** 1611–1620 (1984).
6. A. Bejan and R. Anderson, Natural convection at the interface between a vertical porous layer and an open space, *J. Heat Transfer* **105,** 124–129 (1983).
7. T. Nishimura, T. Takumi, M. Shiraishi, Y. Kawamura and H. Ozoe, Numerical analysis of natural convection in a rectangular enclosure horizontally divided into fluid and porous regions, *Int. J. Heat Mass Transfer* **29,** 889–898 (1986).
8. S. Mori, M. Kataya and A. Tanimoto, Performance of counterflow, parallel plate heat exchangers under laminar flow conditions, *Heat Transfer Engng* **2,** 28–38 (1980).
9. T. T. Kao, T. Domoto and H. G. Elrod, Free convection along a nonisothermal vertical flat plate, *J. Heat Transfer* **99,** 72–78 (1977).
10. A. E. Zinnes, The coupling of conduction with natural convection from a vertical flat plate with arbitrary surface heating, *J. Heat Transfer* **92,** 528–535 (1970).
11. E. M. Sparrow, Laminar free convection on a vertical plate with prescribed non-uniform wall heat flux or prescribed non-uniform wall temperature, NACA Technical Note 3508 (1955).

TRANSFERT THERMIQUE CONJUGUE ENTRE DEUX CONVECTIONS NATURELLES SEPAREES PAR UNE PLAQUE VERTICALE

Résumé—Le couplage thermique entre deux convections naturelles laminaires séparées par une paroi verticale conductive est étudiée théoriquement en prenant en compte la conduction thermique bidimensionelle dans la paroi de séparation. Des solutions numériques des champs de température dans les deux fluides sont combinées avec la solution analytique pour la paroi, de façon à satisfaire la continuité de la température et du flux thermique des deux cotés de la paroi conductrice. Les résultats obtenus sur le champ entier de température montrent que l'effet de conduction longitudinale dans la paroi est important quand la paroi est épaisse ou avec une conductance thermique élevée ; cette conduction longitudinale relaxe l'interférence entre les deux convections. Des expériences sont conduites pour des systèmes air–air avec une paroi en aluminium ou en verre. Les prédictions théoriques décrivent bien les distributions de température expérimentales et elles montrent la validité de la présente analyse.

KONJUGIERTER WÄRMETRANSPORT ZWISCHEN ZWEI DURCH EINE SENKRECHTE PLATTE GETRENNTEN NATÜRLICHEN KONVEKTIONSSTRÖMUNGEN

Zusammenfassung—Es wird der gekoppelte Wärmetransport zwischen zwei Systemen mit laminarer natürlicher Konvektion theoretisch untersucht, die durch eine wärmeleitende senkrechte Platte getrennt sind. Dabei wird der zweidimensionale Wärmetransport in der Platte berücksichtigt. Um die Kontinuität von Temperatur und Wärmestromdichte beiderseits der leitenden Wand zu befriedigen, werden die numerischen Lösungen für die Temperaturfelder in den beiden Fluiden mit der analytischen Lösung für die Platte kombiniert. Die berechneten Temperaturfelder zeigen, daß die axiale Wärmeleitung in der Platte signifikant wird, wenn die Platte dick ist und eine hohe Wärmeleitfähigkeit aufweist. Außerdem zeigt sich, daß die axiale Wärmeleitung die gegenseitige Beeinflußung der beiden Konvektionsströmungen vermindert. Experimente wurden für Luft/Luft-Systeme und Aluminium oder Glas als Trennfläche durchgeführt. Die theoretischen Berechnungen können die experimentell ermittelten Temperaturverläufe sehr gut vorhersagen und somit die Richtigkeit der durchgeführten Untersuchungen belegen.

СОПРЯЖЕННЫЙ ТЕПЛОПЕРЕНОС МЕЖДУ ДВУМЯ ЕСТЕСТВЕННОКОНВЕКТИВНЫМИ СИСТЕМАМИ, РАЗДЕЛЕННЫМИ ВЕРТИКАЛЬНОЙ ПЛАСТИНОЙ

Аннотация—Проводится теоретический анализ совместного теплопереноса между двумя системами ламинарной естественной конвекции, разделенными вертикальной проводещей стенкой при учете двумерной теплопроводности в ней. Для достижения постоянства температуры и теплового потока на обеих сторонах стенки численные решения температурных полей для обоих потоков жидкостей сочетаются с аналитическим решением для стенки. Полученные результаты для всего температурного поля показывают, что эффект осевой проводимости в стенке является существенным и высоким в случае толстой стенки, и что он также ослабляет взаимодействие между двумя конвекциями в обеих жидкостях. Проведены эксперименты для систем воздух–воздух с проводящей стенкой, выполненной из алюминия или стекла. Теоретические расчеты хорошо описывают экспериментальные распределения температуры, что доказывает справедливость настоящего анализа.